Supplementary Information

Gel polymer electrolyte functionalized separator for high-performance lithium-sulfur batteries

Zhan Fang [a,b], Jian Tan [a,b], Longli Ma [a,b], Pengshu Yi [a,b], Wenyi Lu [a,b], Yuyu Xu [c], Mingxin Ye [a]*, Jianfeng Shen [a,b]*

[a] *Institute of Special Materials and Technology, Fudan University, Shanghai 200433, China*

[b] *Department of Materials Science, Fudan University, Shanghai, China*

[c] *Shanghai Pinghe School, Shanghai, China*

[*] *Corresponding Authors: mxye@fudan.edu.cn; jfshen@fudan.edu.cn*

Experimental section

Materials

Tris(pentafluorophenyl)borane (TPFPB, 97%) and poly(ethylene oxide) (PEO, $M_v =$ 100,000) were purchased from Aladdin. Sulfur (S, 99.5%), lithium sulfide (Li$_2$S, 99.9%) and acetonitrile (99.0%) were obtained from Sinopharm. Carbon nanotube (CNT, 99%) and commercial aluminum oxide/polyethylene (Al$_2$O$_3$/PE) separator were bought from Guangdong Canrud New Energy Technology Co., Ltd, China. N-methyl-2-pyrrolidinone (NMP, 99.9%), polyvinylidene fluoride (PVDF, Mv=1,000,000), 1, 3-dioxopentylene (DOL), 1, 2-dimethyl ether (DME) and 1 M lithium bis-(trifluoromethanesulfonyl)imide (LiTFSI) in a mixture of DME: DOL were bought from Suzhou Dodochem Co., Ltd, China.

Preparation of modified separators

Firstly, pre-weighed amount of TPFPB and PEO was dissolved in acetonitrile to form a homogeneous and transparent liquid precursor. The mass concentration of PEO in acetonitrile is 5 mg mL^{-1}, and the mass concentration of TPFPB is 45 mg mL^{-1}. The precursor was then transferred onto one side of a commercial Al$_2$O$_3$/PE separator via blade coating, and the thickness of precursor solution coated on the separator was normalized to 50 μm throughout the experiments, as was controlled by the gap of the coating blade. After volatilizing acetonitrile by natural drying under argon protection, solid TPFPB was reprecipitated on the surface of Al$_2$O$_3$ to form the trilayer composite separator (TPFPB/Al$_2$O$_3$/PE).

Preparation of Li$_2$S$_6$ solution

S and Li$_2$S at a ratio of 1:5 by molar and 1 M LiTFSI in DME: DOL as the solvent were mixed, followed by vigorous stirring at 70°C for 48 h to obtain a Li$_2$S$_6$ solution. The whole operation was carried out in an argon-filled glovebox (H$_2$O <0.1 ppm, O$_2$ <0.1 ppm).

Preparation of S cathode

CNT/S composite nano-material was prepared by employing a melt diffusion method. Firstly, the CNT was mixed with S powder with mass ratio of 3:7, which were sealed in a Teflon pot filled with argon and heated at 160 °C for 12 h to obtain CNT/S nanocomposite material. Then, cathode slurry was prepared by grinding CNT/S and PVDF at a ratio of 9:1 by weight, with NMP as solvent. The cathode slurry was coated on carbon-coated aluminum foil. The as-obtained S cathodes were dried under vacuum for 24h at 60 °C to remove the NMP solvent and obtain the cathode. The cathode was cut into small disc of 12 mm. The S mass loading is 1.0-1.5 mg cm^{-2}. The cathodes with an S mass loading of 4mg cm^{-2} were also prepared.

Materials characterization

The Fourier transform infrared (FT-IR) spectra were recorded using the FTIR microspectroscopy (Nicolet iS50, Thermo Fisher). X-ray photoelectron spectroscopy (XPS) data were obtained on the Scientific K-Alpha electron spectrometer (Thermo Fisher). The morphology and microstructure of the samples were investigated by the scanning electron microscope (SEM, TESCAN MIRA4) at 10 kV. The Nuclear

magnetic resonance (NMR) spectra were obtained on a Bruker AVANCE instrument (500 MHz).

Electrochemical measurements

The CR2025-type coin cells were assembled in an Ar-filled glove box. For the Li-S full cells, 30 μL of the liquid electrolyte precursor (1 M LiTFSI in DME: DOL=1:1 Vol%) was added in the preassembled cell that contains S cathode, Al_2O_3/PE separator or TPFPB/Al_2O_3/PE separator, Li metal anode. The cells were then sealed and rested for 12 h till the polymerization was completed. A LAND CT2001A battery testing system was used to measure the galvanostatic charge/discharge of Li-S coin cells. The galvanostatic cycling tests were carried out between 1.7 and 2.8 V at various current densities. The C-rate for Li-S coin cell tests were ranged from 0.1C to 3C, in which 1C is defined as 1675 mA g^{-1} for S based on the mass of S elements only.

The ionic conductivity (σ, mS cm^{-1}) of the separator was obtained by electrochemical impedance spectra (EIS) on a CHI660E electrochemical instrument and was calculated by equation 1:

$$\sigma = \frac{L}{R_b S}$$

(1)

where L (cm) is the thickness of the separator, R_b (Ω) is the bulk electrolyte resistance, and S (cm^2) represents the area of the separator. The ionic transference number (t_{Li}^+) was measured by combining the direct current (DC) polarization with the alternating current (AC) impedance method with a polarization voltage of 10 mV at room temperature. The t_{Li}^+ value can be calculated by equation 2:

$$t_{Li^+} = \frac{I_S(\Delta V - I_0 R_0)}{I_0(\Delta V - I_S R_S)}$$

(2)

where ΔV stands for the potential applied to the cell, I_0 and R_0 are the initial current and interfacial resistance, while I_S and R_S represent the steady state current and interfacial resistance, respectively. The electrochemical stability was investigated by linear sweep voltammetry (LSV) and the potential ranged from 0 to 6 V. All the electrochemical measurements were performed under room temperature.
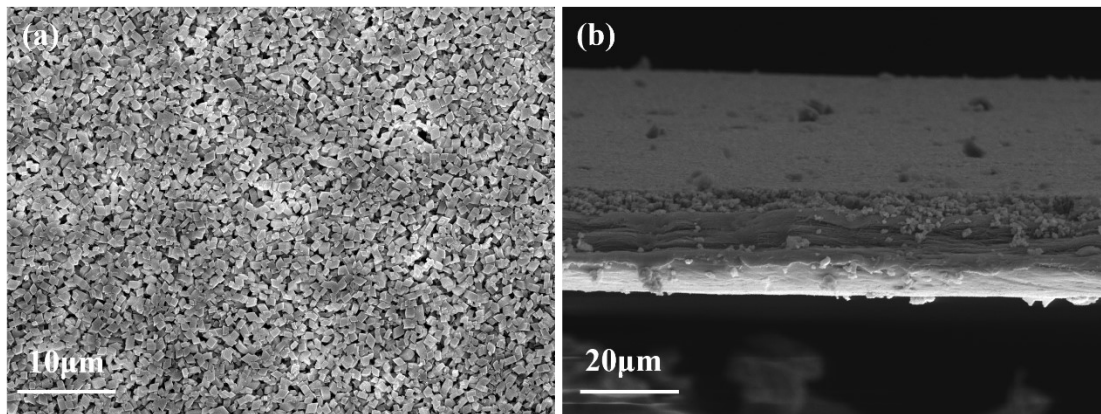
Fig. S1. SEM image of (a) top and (b) cross-section of Al$_2$O$_3$/PE separator.
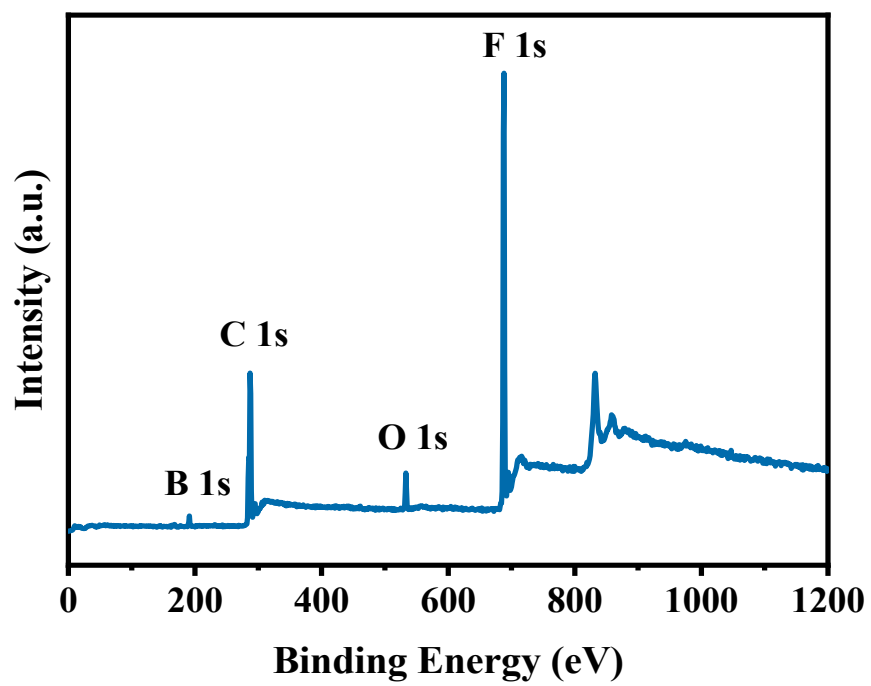
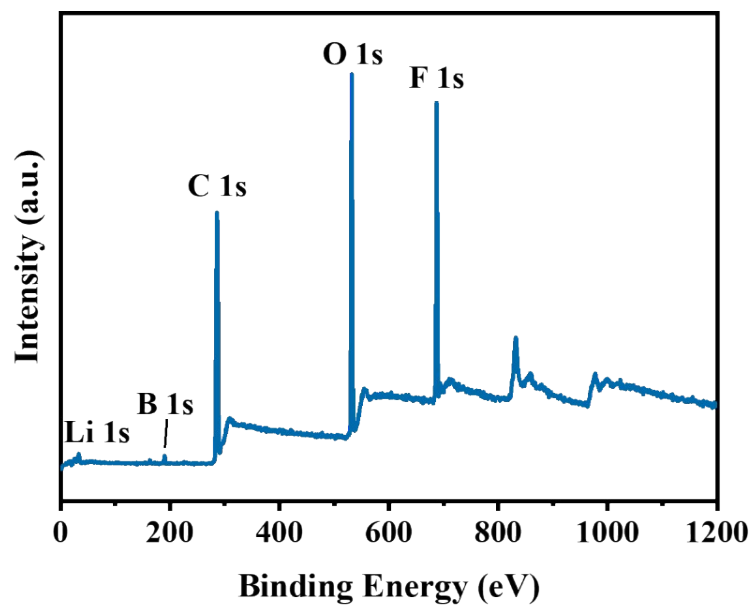**Fig. S2**. XPS spectra collected from the surface of the functional separator.

TPFPB/Al$_2$O$_3$/PE separator → **DME/DOL Infiltration** → **DME/DOL Polymerization**
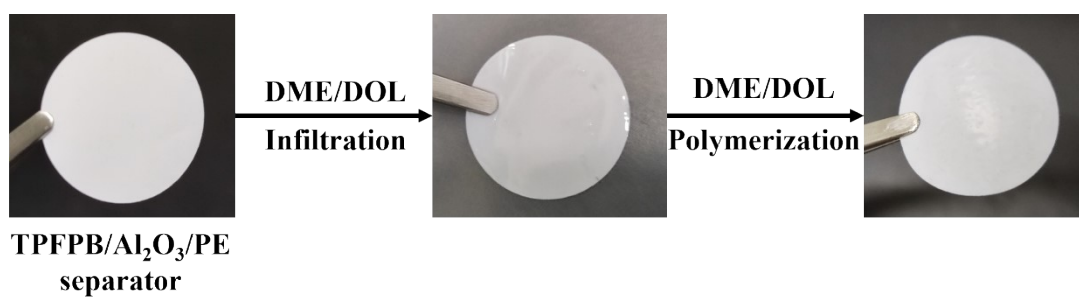
Fig. S3. Optical photograph of the formation of a gel blocking layer on the surface of separator.

Fig. S4. XPS spectra collected from the gel layer formed on the surface of functional separator.
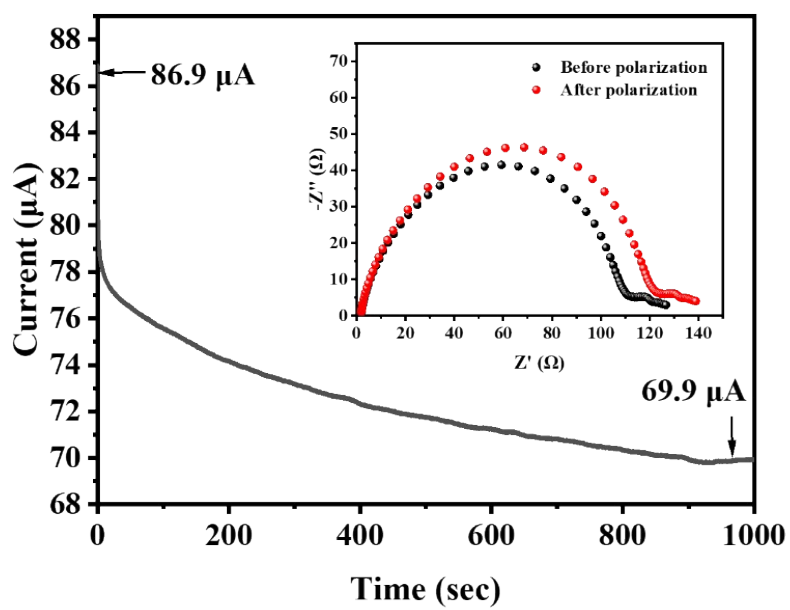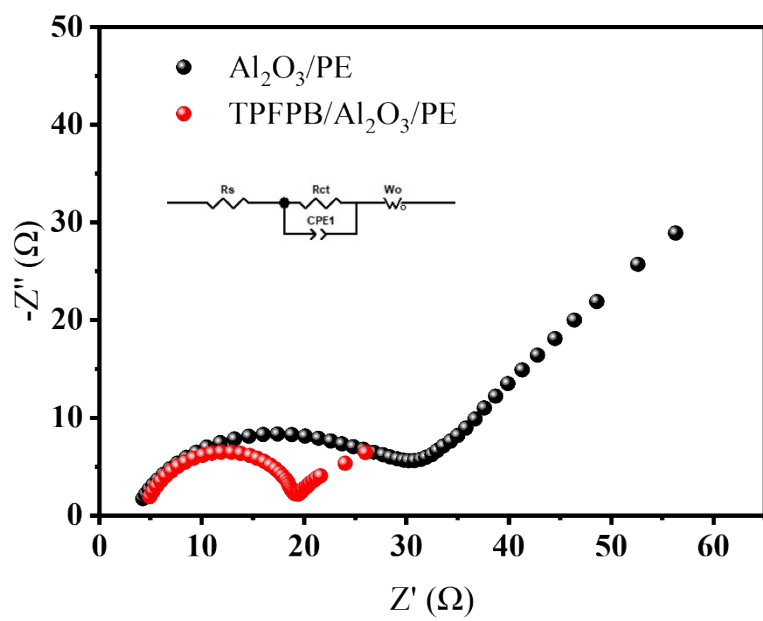
Fig. S5. Li$^+$ transference of Al$_2$O$_3$/PE separator.

Fig. S6. EIS of Al$_2$O$_3$/PE and TPFPB/Al$_2$O$_3$/PE separator for Li-S batteries.
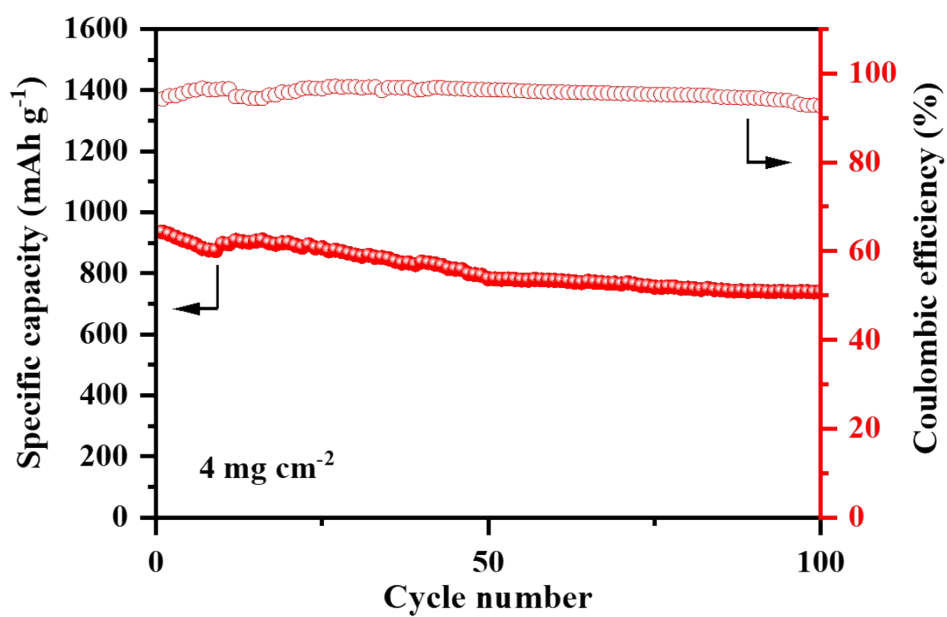
Fig. S7. Cycling performance at 0.2 C of the Li-S cells with the TPFPB/Al$_2$O$_3$/PE separator and high S loading cathode of 4 mg cm^{-2}.

Table S1. Quality change of TPFPB/Al_2O_3/PE separator before and after modification.

	a	b	c	d	e	Average
TPFPB/Al_2O_3/PE separator (mg)	3.06	3.09	3.05	3.07	3.08	3.07
Al_2O_3/PE separator (mg)	2.92	2.92	2.92	2.92	2.92	2.92
TPFPB+PEO (mg)	0.14	0.17	0.13	0.15	0.16	0.15

The sum of the mass of TPFPB and PEO coated on the commercial Al_2O_3/PE separator was calculated to be 0.15 mg based on the average value. Since the TPFPB added during the preparation of slurry in the process of preparing modified separator accounted for 90% of the total mass of TPFPB and PEO, the average mass of TPFPB contained on a single modified separator was 0.135 mg, or 0.000264 mmol. Based on the results of the previous cross-sectional SEM characterization, the thickness of the coating layer is 10 μm, and therefore, for a modified separator with a 19-mm diameter, if the entire surface of the coated layer is filled with liquid electrolyte, it will require 0.003 mL of the electrolyte. Therefore, the concentration of TPFPB in the area of the coating layer was calculated as 0.000264 mmol/0.003 mL = 0.088 mmol mL^{-1}.

Table S2. The comparison of electrochemical performances at similar conditions with commercial separators.

	Ionic conductivity (mS cm^{-1})	Ionic transference number	Electrochemical Window (V)	Initial capacity (mA h g^{-1}, at 0.5 C)	final capacity (mA h g^{-1}, after 500 cycles)	Capacity retention (%)
Al$_2$O$_3$/PE	0.93	0.25	4.4	799	390	48.8
TPFPB/Al$_2$O$_3$/PE	1.22	0.66	4.8	956	664	69.5

Table S3. The comparison of electrochemical performances of Li-S batteries with different modified separators.

modified separators	Sulfur loading (mg cm^{-2})	Initial capacity (mA h g^{-1})	C rate	Cycles	Decay rate (%)	references
MOF/Nafion/PP	1.0	680	0.5	300	0.07	[1]
PEI/PDA/PP	0.45-0.59	1250	0.2	100	0.28	[2]
Carbon/PP	1.0	1198	0.3	100	0.42	[3]
Ti$_4$O$_7$/CNT/PE	3.5	888	0.5	250	0.1	[4]
KB/N/ZnO/PE	3	868	0.5	400	0.1	[5]
TPFPB/Al$_2$O$_3$/PE	1-1.5	956	0.5	500	0.06	This work

References

1. W. Diao, D. Xie, D. Li, F. Tao, C. Liu, H. Sun, X. Zhang, W. Li, X. Wu and J. Zhang, *Journal of Colloid and Interface Science*, 2022, **627**, 730-738.
2. C. Pei, J. Li, Z. Lv, H. Wang, W. Dong and Y. Yao, *International Journal of Energy Research*, 2021, **46**, 10099-10110.
3. J. R. Choi, E. Kim, B. I. Park, I. Choi, B. H. Park, S. B. Lee, J. H. Lee and S. Yu, *Journal of Industrial and Engineering Chemistry*, 2022, **115**, 355-364.
4. X. Wu, S. Li, S. Yao, M. Liu, S. Pang, X. Shen, T. Li and S. Qin, *International Journal of Energy Research*, 2020, **45**, 4331-4344.
5. X. Qian, J. Cheng, L. Jin, Y. Wang, B. Huang and J. Chen, *Colloids and Surfaces A: Physicochemical and Engineering Aspects*, 2022, **648**.